ELSEVIER

Brain Research 881 (2000) 9–17

BRAIN RESEARCH

www.elsevier.com/locate/bres

Research report

Temporal changes in neuronal dropout following inductions of lithium/pilocarpine seizures in the rat

Oksana Peredery, M.A. Persinger*, Glenn Parker, Leon Mastrosov

Neuroscience Laboratory, Departments of Psychology and Biology, Laurentian University, Sudbury, Ontario, Canada P3E 2C6

Accepted 18 July 2000

Abstract

Estimates of neuronal dropout for approximately 100 structures as defined by Paxinos–Watson were completed for brains of male Wistar albino rats between 1 and 50 days after status epilepticus was evoked by a single systemic injection of lithium and pilocarpine. Sample estimates of neuronal loss were strongly correlated with direct measures of cell density. The most extensive immediate damage occurred within the substantia nigra reticulata, CA1 field of the hippocampus, the piriform cortex and the reuniens and paratenial nuclei of the thalamus. Neuronal dropout continued in many other structures over a 50-day period. Structures that showed the greatest 2-deoxyglucose (2-DG) uptake during discrete seizures and waxing and waning seizures within the early stages of status epilepticus but the least 2-DG uptake at the time of late continuous spiking and fast spiking with pauses [Neuroscience 64 (1995) 1057, 1075] exhibited the most neuronal dropout. Relationships between the delay of injection of acepromazine (which facilitated survival) and the amount of damage suggested that the source of the process that results in permanent brain damage may originate within the region of the piriform cortices and its subcortices. © 2000 Elsevier Science B.V. All rights reserved.

Keywords: Thalamus; Lithium; Muscarinic effect; Brain region; Acepromazine; Seizure; 2-Deoxyglucose

1. Introduction

The induction of limbic seizures by the systemic injection of 3 mEq/kg of lithium chloride and 30 mg/kg of pilocarpine [10] produces intractable electrical activity that results in excitotoxic or (delayed) apoptotic death within all structures that were functionally associated with the structures in which the seizures originated. We have been able to measure these histopathological changes months after the induction of status epilepticus [11,20,22] because a single subcutaneous injection of acepromazine within 30 min after the onset of the overt motor component of the seizure reduces the 48-h mortality from more than 90% to less than 20% [7].

The present experiments were designed: (1) to discern which structures exhibited histopathological changes over the 50 days following the induction of the status epilepticus, and (2) to compare the estimates of neuronal losses within these structures with their metabolic activity during the first few hours after the induction of the seizures, as reported by other researchers [5,6]. We reasoned that if the neuronal losses following this model of lithium/pilocarpine-induced seizures were robust and generalizable, our measures of neuronal damage should be correlated significantly with metabolic indicators measured by other researchers for a different sample of rat brains.

2. Materials and methods

2.1. Animals and treatment

A total of 72, 90 to 120 day old male Wistar albino rats, obtained from Charles River (Quebec) were selected as subjects. All rats were injected subcutaneously with 3 mEq/kg of lithium chloride and then either 4 or 24 h later with 30 mg/kg of pilocarpine. The rats whose brains were used in the major study ($n = 62$) were injected 1 h after the injection of the pilocarpine (about 30 min after the onset of the forepaw clonus) with 25 mg/kg of acepromazine (Atravet). Overt signs of status epilepticus were reduced but not eliminated.

Between 1 and 50 days after the onset of the seizure, the

*Corresponding author. Behavioral Neuroscience Program, Laurentian University, Sudbury, Ontario, Canada P3E 2C6. Tel.: +1-705-675-4824/4826; fax: +1-705-671-3844.

E-mail address: mpersinger@admin.laurentian.ca (M.A. Persinger).

0006-8993/00/$ – see front matter © 2000 Elsevier Science B.V. All rights reserved.
PII: S0006-8993(00)02730-X

rats were decapitated. The cerebrums were removed within 5 min, fixed in ethanol–formalin–acetic acid (EFA), and processed according to established procedures [18]. Coronal, 10 μm sections were selected every 200 μm between the caudal mesencephalon and the anterior commissure. Each section was stained with toluidine blue O. This fixation and staining produced very sharp histomorphological detail that we have found clearer and more consistent than fixation in 10% formalin (buffered or not) and staining with other basophilic dyes.

2.2. Micromorphology and quantification

The total area of each coronal section for each rat was evaluated by light microscopy at 100× and 400×. Each of the structures, as defined by Paxinos and Watson [16], was assessed according to an ordinal ranking scale; successively higher scores were used to infer more extensive damage. Construct validity of this measure had been suggested by the strong (0.80) correlation between quantitative values for damage within the medial dorsal thalamic nucleus and the severity of behavioral deficits in different types of radial arm mazes [8].

The scale was constructed as follows: 0, no discernable damage; 1, diffuse neuronal dropout; 2, multiple areas of cystic lesions (e.g., no cells or a fine reticular fiber network); 3, pervasive distribution of small dark Nissl-staining grains (1 to 10 μm); 4, larger aggregates of dark staining Nissl material (>1 mm diameter and sometimes involving the entire structure); and 5, crystalline formations of aggregates of this material which have been shown by atomic absorption and histochemistry to contain dense concentrations of calcium [11]. Two measures were obtained for each structure: (1) the percentage of brains (animals) that displayed only neuronal dropout, and (2) the percentage of brains that displayed any form of neuronal (sum of Type 1 to Type 5) damage.

To verify that our qualitative measures by visual inspection were valid, neuronal densities were determined for each of 10 thalamic nuclei from each of 10 brains randomly selected from the 62 brains. Thalamic structures were selected because of their spatial proximity and easily identifiable neurons. The numbers of cells per grid (hand counted) were counted at 1000× for between 5 and 10 fields per thalamic nucleus by moving through successively adjacent fields from left to right within the boundaries (determined at 40×, 100×) of the nucleus. The mean of these measures constituted the value for the structure. In addition, the same 10 thalamic structures were evaluated for four normal, male, age-matched rats.

These quantitative measures were completed by the fourth author who was not familiar with the treatment history of the rats. Percentage of neuron loss for each thalamic nuclei was calculated by dividing the mean of the cell densities (for the 10 rats) for each nucleus by the mean of the control values for that structure, subtracting from 1, and multiplying by 100. The level of statistical significance and the effect size (η^2) between the measures from brains in which seizures had been induced and the reference brains were obtained by analysis of variance.

2.3. Temporal differences

Our previous quantitative analyses of this type of brain damage and the correlative behavioral changes in the rats [14] had suggested two significant inflection times: the first occurred between postseizure days 10 and 18–20 days, when rats began to display many of their bizarre behaviors such as increased aggression [3] and persistent gnawing [2]. The second time occurred after 30 to 35 days, when the progressive (lateral) ventricular dilatation [22] that had been evident since postseizure day 5 had approached an asymptote and the crystalline formations aggregated into large discernable masses [11].

To test the hypothesis that neuronal loss or changes could emerge (or become apparent) in different structures after the initial damage from the seizure induction, χ^2 analyses ($P < 0.05$, which was equivalent to a ϕ correlation >0.40) for the nominal measure of neuronal dropout were completed for the brains of rats that were killed during specific intervals after the induction of the seizures. The intervals, which had been selected on the bases of the qualitative changes in behavior we had observed during our original studies [21,22], were: (1) 1 through 5 days ($n = 15$) vs. 10 days ($n = 16$) postseizure, (2) 1 through 10 days vs. 15 through 18 days ($n = 15$) postseizure, and (3) 1 through 18 days vs. 50 days ($n = 16$) postseizure induction. For the latter comparison the measure of the sum of the different types of damage was calculated (because of the possibility that accretion of the *G* factor could occur without continued neuronal dropout) and evaluated by one-way analysis of variance.

2.4. Comparison with 2-DG measures from other studies

To discern which stages of electrical activity, as defined by Handforth and Treiman [5,6], were associated with the subsequent cell loss in various nuclei, the values for the amount of glucose uptake for rats (not involved in our present study) from their two papers was obtained for the 28 distinct telencephalic and diencephalic structures that were common to both their studies and our study. Spearman ρ and Pearson r correlations were calculated between our measures of neuronal dropout or total damage and the values from Handforth and Treiman [5,6] for the local cerebral glucose utilization during the early stages and late stages of status epilepticus. To identify shared sources of variance, exploratory factor analyses (PA1) were performed for the 2-DG measures associated with each of the five electrical stages designated for the early stage of the seizure and the two measures of damage in our study and for the 2-DG levels for each of the seven electrical states

for the later stages of the status epilepticus and the two measures of damage in our study.

2.5. Latency before injection of acepromazine

To assess if the injection of acepromazine was instrumental in the stabilization of the seizure-induced brain damage, an additional 10 rats were injected with acepromazine between 0 and 6 h after the injection of the pilocarpine. These rats were killed 48 h later; the brains were removed and processed as specified earlier. Bivariate correlations (Pearson *r*) were completed for the time (in h) between the pilocarpine–acepromazine injections and the amount of total damage within each structure. All statistical analyses involved SPSS software on a VAX 4000 computer.

3. Results

3.1. Qualitative patterns

Different types of neuronal damage dominated different regions of the diencephalon and telencephalon following the induction of status epilepticus by lithium and pilocarpine. Only the reticulata component of the substantia nigra (SNR) was damaged within the mesencephalon. Neuronal dropout and diffuse gliosis was found in many regions of the thalamus, amygdala, SNR, hippocampus and basal ganglia. The neuropathology within the SNR was always located in the lozenger-shaped region that receives thalamic inputs. After about 20 days following the seizure induction, there was minimal gliosis and maximal neuronal dropout within this region.

Severe neuronal loss and gliosis were found almost always within the CA1 region of the hippocampus (Fig. 1). Within the amygdala, neuronal dropout and gliosis were distributed diffusely throughout specific nuclear structures while other structures, such as the central group, were not affected. Near-complete neuronal dropout, with cystic lesions, was found only within the limbic cortices such as the entorhinal and piriform regions (Fig. 2).

Neuronal dropout and gliosis occurred within 10 days of the seizure induction in most structures. After about 20 days, within many thalamic nuclei, a second phenomenon evolved. Darkly staining Nissl material was accumulated

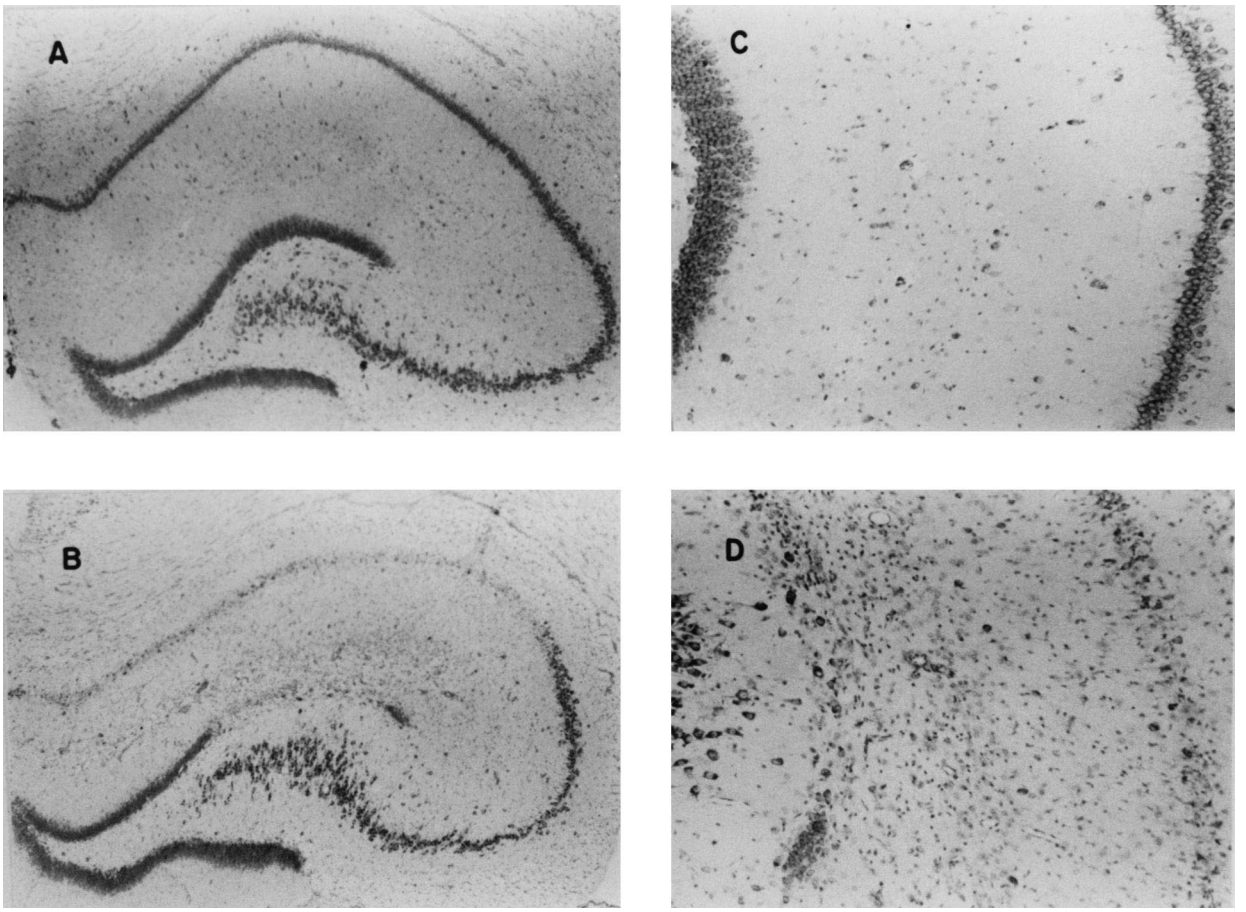

Fig. 1. Photomicrograph (40×) of the hippocampal formation (Ammon's Horn) for a control (A) and for a rat in which lithium/pilocarpine seizures had been induced (B) showing loss of neurons in the dentate gyrus and CA1. Section C (100×) shows the cells within the dentate gyrus (left) and CA1 (right) for a normal rat, while Section D (100×) shows their absence in the brain of a seized rat.

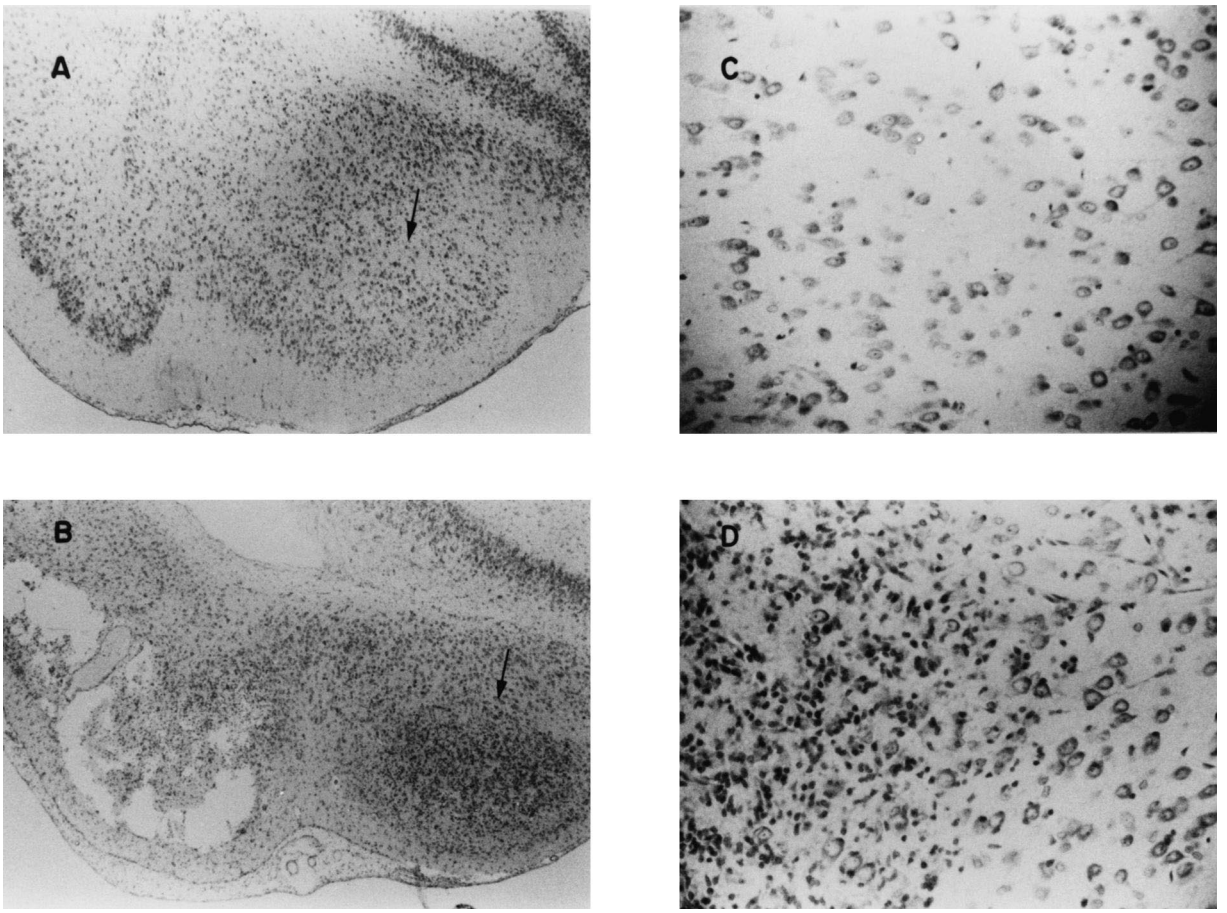

Fig. 2. Photomicrographs (40×) of the entorhinal cortices (below the A) and the amygdala (arrow) for a control brain and of the entorhinal cortices with cystic lesions (below the B) and the amygdala (arrow) for a seized brain. The gliosis within the amygdala of the seized brain (D, 100×) is not evident in the amygdala (C, 100×) of the normal brain.

within discrete thalamic structures. By postseizure day 50, these diffuse bluish areas slowly resolved into dense formations; about half of them displayed crystalline characteristics (Fig. 3) which were similar to those shown [11] to contain dense calcium deposits embedded within a mucopolysaccharide matrix.

3.2. Semiquantitative patterns over time

The percentages of brains ($n = 62$) that displayed any discernable neuronal dropout within the amygdala, thalamus, and other structures are shown in Table 1. The total damage score, defined as the sum of all types of damage, for each structure is also shown. Within the amygdala the neuronal dropout occurred most frequently (>70% of the brains) within the posterior, lateroventral and basomedial groups. The central nucleus was never observably damaged.

The thalamic structures displayed a marked variability in the severity of damage. Structures that displayed the most frequent neuronal dropout included most of the mediodorsal group, the lateral and posterior nuclei and the regions around and including the suprageniculate nucleus. The reuniens and paratenial nuclei of the thalamus deserve special attention because of their extremely frequent (>90%) devastation of neuronal populations. The least (>2% but <15%) damaged structures were the ventral portions of the lateral and medial geniculate, the reticular nucleus and the limbic thalamic nuclei. Neocortices showed a moderate (40%) frequency of damage; the temporal and parietal cortices were damaged significantly ($P < 0.05$) more often than the frontal, occipital, insular or perirhinal cortices. There was almost total neuronal dropout within the piriform, retrosplenial, and entorhinal cortices.

Neuronal dropout (primarily pyramidal cells) was most extreme within the CA1 sector of the hippocampal formation. This type of damage decreased progressively within the CA2, CA3 and CA4 regions, respectively. Moderate incidences of damage occurred within the subiculum and dentate gyrus. Other subcortical telencephalic structures that displayed similar damage involved the claustrum, lateral septal nucleus (dorsal part) and the globus pallidus. The incidence of neuronal dropout within the ventral

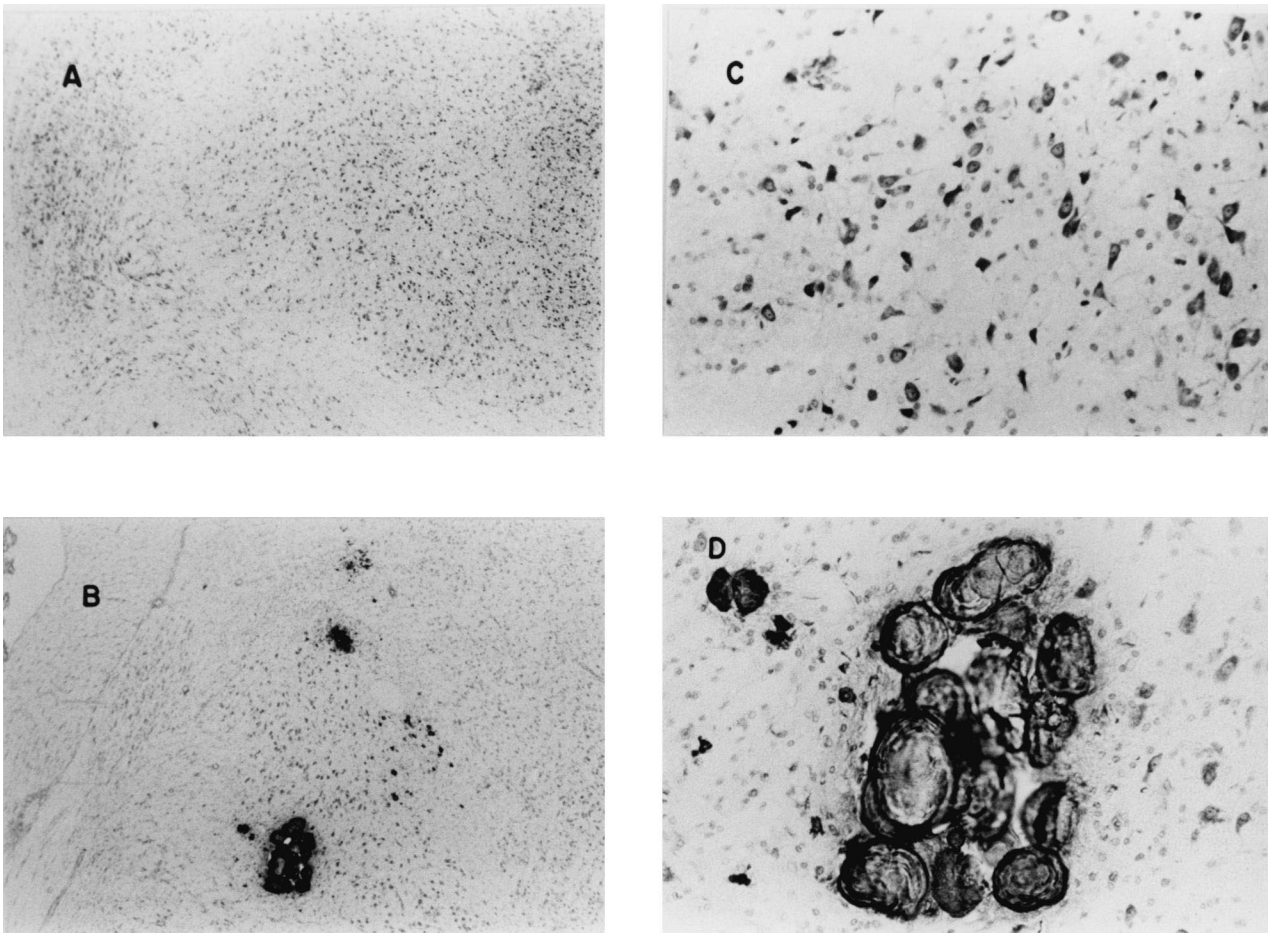

Fig. 3. Photomicrographs (40×) of the lateral portion of the thalamus in a control brain (A) and a brain (B) in which seizures had been induced about 50 days previously. The largest aggregate of crystalline material noted in B is magnified (100×) in D. For comparison, a comparable area of the thalamus is magnified (100×) in the control brain.

striatum was sparse, while the dorsolateral region which represents the forelimbs displayed discernable cell dropout; the entopeduncular nucleus was mildly affected but there were no discernable changes within the nucleus accumbens, substantia innominata, and the region surrounding and including the Islands of Calleja.

Table 2 shows only those structures that displayed postseizure, time-dependent changes in the incidence of neuronal dropout between postseizure days: (a) 1 through 5 vs. 10, (b) 1 through 10 vs. 15 through 18 and (c) 1 through 18 vs. 50. A '+' refers to an increased incidence of neuronal dropout, while a '−' refers to a decrease; the criterion was a ϕ coefficient of greater than 0.40 ($P < 0.05$); a '0' reflects no statistically significant change. In general, the results suggested little additional dropout between days 1 through 5 and days 10 (after the first stage of pathology which was evident within 24 h).

However, between postseizure days 10 and 18, when most of the peculiar rat behaviors began to emerge [2,3,17,19–21], there were conspicuous increases in neuronal dropout within the lateral (LaVM, LaVL) and medial (Me) amygdaloid groups, the medial geniculate group (MGD, MGM) and the centrolateral, gelatinosus and gustatory nuclei of the thalamus. Enhanced dropout was evident within the occipital, temporal, frontal, perirhinal, insular (agranular) and cingulate cortices and within several subcortical telencephalic structures; damage within the CA3 region during this period was notable. The only conspicuous increase in anomalous histomorphology that occurred between postseizure days 1 through 20 vs. day 50 was evident for the total damage score and involved for the most part those structures in which aggregates of calcium deposits had been observed previously [11] in other brains.

3.3. Quantification and validity of measures

The means and standard deviations for neuronal cell density (cells/mm^2) within 10 thalamic nuclei, that displayed the range in percentage incidence of damage within our population of brains, are shown in Table 3. Means and standard deviations for control brains are also indicated as well as the F-value and the strength of the effect (η^2), i.e. the amount of variance in numbers of neurons explained by the treatment compared to no treatment. The amount of

Table 1
Percentage of brains that displayed neuronal dropout or any form of necrosis within specific structures. Abbreviations are from Paxinos and Watson [16]

Structure	Dropout	Any damage	Structure	Dropout	Any damage
Amygdala			*Thalamus*		
PMCo	84	87	Rh	18	18
AHiPA	34	37	Hb	42	42
PLCo	73	77	Re	92	97
BLP	60	60	VL	55	63
LaDL	44	44	G	45	48
LaVM	74	74	Ang	15	16
LaVL	69	69	IAM	23	23
BLA	18	18	PVA	19	21
CeL	0	0	AM	63	71
I	0	0	AD	10	10
BLV	37	40	AVDM	8	8
BM	69	71	AVVL	21	23
Me	39	39	PT	90	90
ACo	27	27	IAD	19	19
CeM	0	0	MD	68	73
IMG	3	3	CM	47	48
IM	5	5	IMD	48	55
CxA	13	15	*Hippocampal formation*		
AA	5	5	S	44	45
ASTR	23	23	DG	42	44
Thalamus			CA1	92	92
MGD	76	81	CA2	68	68
MGV	11	11	CA3	27	27
MGM	39	40	CA4	11	11
SG	84	87	*Cerebral cortices*		
PoT	15	21	Pir	95	97
PLi	13	15	RSCx	71	73
LPMC	66	68	PRh	39	40
DLG	77	77	Ent	73	85
VLG	2	2	Oc	37	37
Eth	2	3	Par	45	45 (LI, II)
LPMR	73	82	Te	47	47
LPLR	47	63	Fr	37	37
MG	24	34	AI, GI	37	42
Po	76	87	*Other subcortical structures*		
VPM	44	48	DEn	90	90
PF	44	45	VEn	82	85
Rt	0	0	Cl	40	40
VPL	52	53	CPu	61	61
Gu	29	31	LS	35	35
CL	56	66	MS	0	0
VLG	0	0	GP	48	50
LDVL	79	87	EP	24	24
PC	61	66	LOT	8	8
MDL	76	85	BSTI	19	19
VM	84	89	VP	2	2
LDDM	73	79	FStr	6	6
MDC	73	76	*Mesencephalon*		
MDM	77	82	SNR	94	97
			SNC	0	0

Table 2
Structures in which there was a significant change (+, increase; −, decrease) in neuronal dropout or total damage in brains of rats that were killed various times (in days) after seizure induction. Abbreviations are from Paxinos and Watson [16]

Structure	Neuronal dropout			Total damage
	<5 vs. 10	<10 vs. 18–20	<20 vs. 50	<20 vs. 50
Amygdala				
PMCo	+	0	0	0
PLCo	0	−	0	0
BLP	0	0	−	−
LaVM	0	+	0	0
LaVl	0	+	0	0
BLA	−	0	0	0
BM	+	0	0	−
Me	0	+	0	0
Thalamus				
MGD	+	0	0	0
MGV	0	+	0	0
MGM	0	+	0	0
SG	0	0	0	+
PoT	0	+	0	0
PLi	0	+	0	0
DLG	0	0	0	+
LPMR	0	0	0	+
LPLR	0	0	0	+
Po	0	−	0	+
Gu	0	+	0	0
CL	−	+	0	0
LDVL	0	0	0	+
LDDM	0	0	0	+
Hb	+	0	0	0
Re	0	0	0	+
G	0	+	0	0
Cortices				
Oc	0	+	0	0
Te	0	+	−	−
Fr	0	+	−	−
AI	0	+	0	0
Cg	0	+	−	0
Hippocampal formation				
S	0	+	+	0
CA1	+	0	0	0
CA3	0	+	0	0
Other subcortical structures				
Cl	0	+	0	0
CPu	0	+	0	0
LS	0	+	0	0
GP	0	+	0	0

variance in cell loss that could be attributed to the seizures ranged from minimal (rhomboid nucleus) to a maximum of 99% (nucleus reuniens). A correlation (ρ) of 0.86 ($P < 0.001$) existed between the percentages of cell loss (relative to controls) for each of the 10 thalamic nuclei (average of 10 brains) and the proportion of all ($n = 62$) brains that displayed some form of damage.

3.4. Comparisons of 2-DG measures and neuronal dropout

The factor loadings for the 2-DG activity in the 28 shared structures specified in the Handforth and Treiman data [5,6] for the early and late stages of status epilepticus and neuronal dropout for each structure (the mean of the

Table 3
Means and standard deviations for the cellular density of neurons (1×10^3 cells/mm^2) for sample thalamic nuclei. Abbreviations are from Paxinos and Watson [16]

Nuclei	Control		Seizure		F-value	η^2
	M	S.D.	M	S.D.		
PF (L)	1.22	0.06	0.99	0.22	4.70*	0.28
VM	0.47	0.04	0.29	0.13	7.22*	0.38
RH	2.26	0.11	1.94	0.32	3.56	0.23
MD (L)	0.72	0.05	0.12	0.07	242.70***	0.95
LPMC	0.77	0.02	0.12	0.07	303.16***	0.95
VPL	0.51	0.01	0.40	0.08	8.96*	0.43
Re	1.20	0.05	0.05	0.03	2830.86***	0.99
IAM	1.21	0.18	0.28	0.20	66.60***	0.85
AVVL	2.04	0.22	1.30	0.24	27.93***	0.70
VLG	0.99	0.10	0.83	0.07	11.22**	0.48

*$P<0.05$, **$P<0.01$, ***$P<0.001$.

62 brains in our major study) are shown in Table 4. (To be conservative, we accepted only loading coefficients that explained at least 50% of the variance ($r>0.70$) as statistically significant.) The structures that showed the greatest metabolic activation, as inferred by 2-DG, during waxing and waning and discrete spiking electrical seizures also showed the most consistent neuronal dropout in our population of brains.

However, the structures that showed the greatest 2-DG activity during the fast spiking with pauses and late continuous spiking during the later phases of status epilepticus in the Handforth and Treiman study exhibited the least cell loss in our study. The loading coefficients for these variables, when the total damage measures were employed instead of the proportion of neuronal dropout, were similar in magnitude and statistical significance. The statistically significant ($P<0.05$) Pearson r and Spearman ρ correlations (in parentheses, respectively) between the neuronal dropout and the EEG measures were: discrete seizures (0.40, 0.51), late continuous spiking (-0.50, -0.61), fast spiking with pauses (-0.59, -0.63), early PEDs (periodic epileptic discharges) with clonus (-0.40, -0.51) and late PEDs with clonus (-0.46, -0.60).

3.5. Damage and latency of acepromazine injection

The increased incidence and severity of neuronal dropout within the diencephalon and telencephalon as a function of the time (-0.5 to 6 h) between the seizure onset and removal of the brain were qualitatively conspicuous. Statistically significant ($r>0.60$) correlations were evident for the entorhinal cortices, amygdaloid–hippocampal transition area, basolateral nucleus (anterior part) of the amygdala, anteroventral thalamic nucleus (ventrolateral part) and CA3 of the hippocampal formation. The severity of damage rapidly increased when the acepromazine injection was delayed for more than 2 h. Even when acepromazine was injected before the seizure onset (within seconds of the pilocarpine), pervasive neuronal dropout was still discernable within 48 h for all brains for the following structures: piriform cortices, CA1 of the hippocampus, the dorsal and ventral endopiriform nuclei, basolateral nucleus of the amygdala (anterior part), mediodorsal thalamic nuclei (medial and central part), the nucleus reuniens and the reticulata of the substantia nigra.

4. Discussion

The results replicated and extended previous reports that evolving histopathology within the rat brain following a systemic injection of lithium and pilocarpine simulates the patterns of neuronal dropout associated with single, larger dosages of pilocarpine [1,23]. In general, the temporal evolution of the neuronal loss within various diencephalic and telencephalic structures was similar to those that followed limbic status epilepticus evoked by direct electrical stimulation [26].

The results of the present study indicated that neuronal loss may continue beyond the 48-h period, the frequent endpoint in many studies. We measured additional losses of neurons between days 10 and 18 after the induction of seizures. These changes occurred within structures that have been associated with the clear emergence of hyperresponsiveness to sounds, persistent micromovements

Table 4
Factor loadings (r values) after varimax rotation for the amount of damage in Paxinos and Watson-designated structures in the present study and the 2-DG uptake values (subtracted from lithium controls) during various electroencephalographic stages of the early and later phases of status epilepticus from different rats reported by Handforth and Treiman [5,6]

Early phases		Late phases	
Variable	Loading	Variable	Loading
Discrete seizures	0.78	Early continuous spiking	0.06
Waxing and waning	0.73	Late continuous spiking	0.45
Fast and slow spiking	0.40	Fast spiking with pauses	0.86
Early continuous spiking	−0.12	Early PEDs with clonus	0.90
Late continuous spiking	−0.89	Late PEDs with clonus	0.90
Neuronal dropout	0.67	Late PEDs subtle	0.71
		Late PEDs electrical	−0.13
		Neuronal dropout	−0.71

of the pinnae [19,21], aggressive behavior [3,19], attenuated conditioned taste aversion [19,20], remarkably poor spatial maze acquisition [8,20] and loss of maternal behavior [17]. The cause of the neuronal loss, which could include delayed excitotoxic effects, apoptosis, or the consequences of recurrent spontaneous seizures that are displayed by these rats during their lifetimes, must still be discerned.

The specific structures that were damaged and the similar magnitudes of this damage were consistent with results from other techniques [4,12,13,24,25]. For example, the small lozenger-shaped region of damage within the substantia nigra reticulata was the region that receives inputs from the most damaged nuclei of the thalamus. The similar magnitude of the damage within the nucleus reuniens and layers I and III of the entorhinal cortices and the molecular stratum of the CA1 field of the hippocampus would be compatible with the distribution of contributions revealed by horseradish peroxidase [9,27]. Such convergence of results from varied methods may allow discrimination of essential patterns of neuronal loss following hyperactivation of neurons from those artifactual details coupled to specific techniques or procedures.

Although our measures of neuronal dropout were based upon visual discrimination at 100×, the validity of this method was indicated by the strong correlation between actual counts of neurons at 1000× within a random sample of brains and the proportion of rats whose brains displayed this visible (at 100×) damage. Considering the strength of this correlation, we suggest that the results of the factor analyses of the 2-DG data from Handforth and Treiman and our measures of neuronal loss were valid, even as an exploratory procedure. These results indicated that those structures that will exhibit the most neuronal dropout (as inferred in our studies) show the greatest metabolic activity during the discrete seizures and waxing and waning seizures that begin about 30 min after the injection of the pilocarpine. The more recent measurements [15] of *c-fos* expression (a marker of cellular hyperactivity) within the same structures that have shown the greatest 2-DG uptake and cell loss following induction of status epilepticus by lithium and pilocarpine are consistent with this pattern.

That the amount of neuronal loss could be minimized was suggested by the correlation between the amount of neuronal dropout in structures distal to the entorhinal/piriform cortices and its subcortical nuclei and the time before the acepromazine was injected. However, even if the acepromazine was injected at the time of the observable onset of forelimb clonus and its electrical correlates, which usually emerge about 30 min after pilocarpine injection [5,6], the cell losses within the piriform cortices — CA1 — and midline thalamic nuclei were not attenuated. Whether or not prophylactic agents such as acepromazine and ketamine prevent the seizure from spreading from the piriform region to other areas or protect the target structures is not clear.

What was clear, however, is that those structures that displayed the greatest uptake of 2-DG during late continuous spiking and fast spiking with pauses in the Handforth and Treiman study [5,6] displayed less neuronal dropout in our study. If this specific pattern of electrical seizures reflects the changes in inhibitory neurons [25] or metabolic pathways that attenuate excitotoxic consequences within these structures, then one would expect less neuronal dropout due to either necrosis or apoptosis.

Acknowledgements

Thanks to Ayerst Laboratories, Montreal, Quebec, for supplying the acepromazine. This research was supported, in part, by a grant from the Laurentian University Research Foundation. Technical support from C. Blomme and L. Brosseau is appreciated.

References

[1] Y.R.J. Bureau, O. Peredery, M.A. Persinger, Concordance of quantitative damage within the diencephalon and telencephalon following systemic pilocarpine (380 mg/kg) or lithium (3 mEq/kg)/pilocarpine (30 mg/kg) induced seizures, Brain Res. 648 (1994) 265–269.

[2] Y.R.J. Bureau, M.A. Persinger, Transient blocking of persistent gnawing by haloperidol in rats with seizure-induced multifocal brain damage, Life Sci. 52 (1993) 869–876.

[3] D. Desjardins, M.A. Persinger, Association between intermale social aggression and cellular density within the central amygdaloid nucleus in rats with lithium/pilocarpine-induced seizures, Percept. Mot. Skill. 81 (1995) 635–641.

[4] M.J. Dolleman-Van Der Weel, M.P. Witter, Different populations of neurons in the nucleus reuniens thalami project selectively to distinct divisions of the rat hippocampal region, Eur. J. Morphol. 33 (1995) 198.

[5] A. Handforth, D.M. Treiman, Functional mapping of the early stages of status epilepticus: a ^{14}C-2-deoxyglucose study in lithium–pilocarpine model in rat, Neuroscience 64 (4) (1995) 1057–1073.

[6] A. Handforth, D.M. Treiman, Functional mapping of the late stages of status epilepticus in the lithium–pilocarpine model in rat: a ^{14}C-2-deoxyglucose study, Neuroscience 64 (4) (1995) 1075–1089.

[7] T. Harrigan, Y.R.J. Bureau, M.A. Persinger, G.H. Parker, Prevention of sudden cardiac death by the atypical neuroleptic acepromazine following status epilepticus in rats, Life Sci. 54 (24) (1994) PL457–PL462.

[8] T. Harrigan, O. Peredery, M.A. Persinger, Radial maze learning deficits and mediodorsal thalamic damage in context of multifocal seizure-induced brain lesions, Behav. Neurosci. 105 (3) (1991) 482–486.

[9] M. Herkenhan, The connections of the nucleus reuniens thalami: evidence for a direct thalamo–hippocampal pathway in the rat, J. Comp. Neurol. 177 (1978) 589–610.

[10] M.P. Honchar, J.W. Olney, W.R. Sherman, Systemic cholinergic agents induce seizures and brain damage in lithium-treated rats, Science 220 (1983) 323–325.

[11] G.F. Lafreniere, O. Peredery, M.A. Persinger, Progressive accumulation of large aggregates of calcium-containing polysaccharides and basophilic debris within specific thalamic nuclei after lithium/pilocarpine-induced seizures, Brain Res. Bull. 28 (1992) 825–830.

[12] J.E. LeDoux, C. Farb, D.A. Ruggiero, Topographic organization of

neurons in the acoustic thalamus that project to the amygdala, J. Neurosci. 10 (4) (1990) 1043–1054.
[13] A.J. McDonald, Organization of amygdaloid projections to the mediodorsal thalamus and prefrontal cortex: a fluorescence retrograde transport study in the rat, J. Comp. Neurol. 262 (1987) 46–58.
[14] D.C. McIntyre, J.R. Plant, Pyriform cortex involvement in kindling, Neurosci. Behav. Rev. 13 (1989) 277–280.
[15] J. Motte, M.J. da Silva Fernandes, T.Z. Baram, A. Nehlig, Spatial and temporal evolution of neuronal activation, stress and injury in lithium-pilocarpine seizures in rats, Brain Res. 793 (1998) 61–72.
[16] G. Paxinos, C. Watson, The Rat Brain in Stereotaxic Coordinates, 2nd Edition, Academic Press, Orlando, FL, 1986.
[17] O. Peredery, M.A. Persinger, C. Blomme, G. Parker, Absence of maternal behavior in rats with lithium/pilocarpine seizure-induced brain damage: support of MacLean's triune brain theory, Physiol. Behav. 52 (1992) 665–671.
[18] M.A. Persinger, Degranulation of brain mast cells in young albino rats, Behav. Neural Biol. 39 (1983) 299–306.
[19] M.A. Persinger, Y.R.J. Bureau, M. Kostakos, O. Peredery, H. Falter, Behaviors of rats with insidious, multifocal brain damage induced by seizures following single peripheral injections of lithium and pilocarpine, Physiol. Behav. 53 (1993) 849–866.
[20] M.A. Persinger, Y.R.J. Bureau, O. Peredery, Dissociation between conditioned taste aversion and radial maze learning following seizure-induced multifocal brain damage: quantitative tests of serial vs. parallel circuit models of memory, Physiol. Behav. 56 (2) (1994) 224–235.
[21] M.A. Persinger, K. Makarec, J.-C. Bradley, Characteristics of limbic seizures evoked by peripheral injections of lithium and pilocarpine, Physiol. Behav. 44 (1988) 27–37.
[22] M.A. Persinger, O. Peredery, D. Desjardins, A. Eastman, Ventricular dilatation over several weeks following induction of excitotoxic (systemic lithium/pilocarpine) lesions: potential role of damage to the substantia nigra reticulata, Int. J. Neurosci. 94 (1998) 63–74.
[23] W.A. Turski, E.A. Cavalheiro, M. Schwarz, S.J. Czuczwar, Z. Kleinrok, L. Turski, Limbic seizures produced by pilocarpine in rats: behavioral, electroencephalographic and neuropathological study, Behav. Brain Res. 9 (1983) 315–335.
[24] E.H.S. Vulpen, R.W.H. van Verwer, Organization of projections from the mediodorsal nucleus of the thalamus to the basolateral complex of the amygdala in the rat, Brain Res. Bull. 500 (1989) 389–394.
[25] N.Y. Walton, S. Gunawan, D.M. Treiman, Brain amino acid concentration changes during status epilepticus induced by lithium and pilocarpine, Exp. Neurol. 108 (1990) 61–70.
[26] L.E. White, J.L. Price, The functional anatomy of limbic status epilepticus in the rat. I. Patterns of ^{14}C-2-deoxyglucose uptake and fos immunocytochemistry, J. Neurosci. 13 (11) (1993) 4787–4809.
[27] F.G. Wouterlood, E. Saldana, M.P. Witter, Projection from the nucleus reuniens thalami to the hippocampal region: light and electron microscopic tracing study in the rat with the anterograde tracer *Phaseolus vulgaris*-leucoagglutinin, J. Comp. Neurol. 296 (1990) 179–203.